Complementary Sliding Mode Control via Elman Neural Network for Permanent Magnet Linear Servo System

HONGYAN JIN AND XIMEI ZHAO

School of Electrical Engineering, Shenyang University of Technology, Shenyang 110870, China

Corresponding author: Ximei Zhao (zhaoxm_sut@163.com)

ABSTRACT The permanent magnet linear servo system is usually susceptible to uncertainties, such as parameter variations, external disturbances, and friction forces. To address this problem, a complementary sliding mode control (CSMC) via Elman neural network (ENN) was presented in this paper. First, the mathematical model of the permanent magnet linear synchronous motor (PMLSM) with a lumped uncertainty was established. Second, on the basis of the traditional sliding mode control (SMC), CSMC was designed by combining the integral sliding surface with the complementary sliding surface. CSMC is generally used to reduce the chattering phenomenon and, consequently, to improve the tracking performance. However, the values of the switching gain and the boundary layer thickness are difficult to select in CSMC. To deal with this problem, ENN was adopted in the proposed CSMC system to replace the switching control law. Due to its strong learning ability, ENN can estimate the value of the lumped uncertainty and adjust the parameters online, thus further improving the robustness of the system. In addition, to verify the control performance of the proposed method, a digital signal processor (DSP) was implemented as the experimental platform to control the mover of the PMLSM for the tracking of different reference trajectories. The experimental results show that the proposed control strategy not only improves tracking accuracy but also guarantees the robustness of the system.

INDEX TERMS Permanent magnet linear synchronous motor (PMLSM), complementary sliding mode control (CSMC), Elman neural network (ENN), lumped uncertainty, tracking performance, robustness.

I. INTRODUCTION

In manufacturing systems, high precision servo machining field is widely employed in many applications such as semiconductor manufacturing, industrial robots, machine tools and computer numerical control (CNC) [1], [2]. However, as mentioned in [3], the traditional rotary motors equipped with gears and ball screws have the disadvantages of low stiffness, long response time and friction loss, which cannot satisfy the precise specifications of manufacturing processes. Compared with the rotary motors, permanent magnet linear synchronous motor (PMLSM) has a simpler mechanical construction, which can directly generate larger electromagnetic thrust and reduce mechanical loss [4], [5]. Moreover, it can

also improve the frame stiffness of the system and reduce the mechanical friction of the motor [6], [7]. Therefore, PMLSM is suitable for high-performance servo applications.

Although PMLSM can directly obtain the linear motion by eliminating the mechanical structure of the motor, PMLSM is highly affected by the lumped uncertainty such as parameter variations, friction forces and external disturbances. Consequently, the system controller should be robust enough to tolerate these uncertainties [8], [9]. Especially in the fields of CNC with high speed and precision, the requirements of servo system are even higher. In order to eliminate the uncertainties existing in the system and realize high precision servo performance of PMLSM, some researchers have proposed many control strategies, such as sliding mode control (SMC), backstepping control, adaptive control, and other intelligent control including expert control and neural network [10], [11].

The associate editor coordinating the review of this manuscript and approving it for publication was Giambattista Gruosso.

It's well known that SMC has a strong robustness, which is insensitive to system parameter variations, friction forces and external disturbances when the system trajectory reaches and stays on the sliding surface [12]. The design process of SMC consists of two relatively independent parts: sliding surface design and control law design, which can ensure different state trajectories stay on the sliding surface in finite time. However, the robustness of the SMC is guaranteed by using the strategy of a large switching control law. It will lead to chattering phenomenon which is caused by switching function in control law, and chattering may excite the neglected or un-modeled high-frequency dynamics [13]–[15]. Thus, chattering has become the major disadvantage of SMC, the way to reduce chattering becomes a popular research issue.

In [16], [17], integral sliding mode control (ISMC) is used to guarantee the global robustness of the control system, though the chattering is weakened by this method efficiently, the system instability will be caused by ISMC when the system state deviates from the reference trajectories. In [18], [19], a fuzzy sliding mode control (FSMC) method is proposed to reduce the chattering, but when the lumped uncertainty of the nonlinear system is excessive, the method to improve the tracking performance of the system will be out of effect. In [20], [21], a neural network compensation is applied to combine with SMC to further optimize the performance. In [22], an adaptive backstepping fuzzy SMC strategy is developed to approximate the upper bound of lumped uncertainties and adjust the unknown parameters online. By introducing complementary generalized error transformation, Su and Wang proposed a complementary sliding mode control (CSMC) to replace the switching function of SMC to improve the tracking precision and reduce chattering in [23]. In [24], CSMC is designed to improve the tracking performance and the robustness of the PMLSM servo system. However, the values of switching gain and boundary layer thickness are difficult to select, only through trial and error method can the appropriate parameters be selected. To solve the problem of parameter selection, Lin proposed an intelligent CSMC which combines the CSMC with RBFNN in [25], RBFNN is used to estimate the lumped uncertainty. However, RBFNN is a static neural network and it is easy to occur local optimization problems.

In this paper, a complementary sliding mode control (CSMC) via Elman neural network (ENN) is proposed to improve the performance of permanent magnet linear servo system. By establishing the dynamic mathematical model of PMLSM with a lumped uncertainty including parameter variations, external disturbances and others, CSMC is designed on the basis of SMC to suppress the influences of uncertainties, thereby reducing the chattering phenomenon and achieving excellent performance. However, the values of the boundary layer and switching gain in CSMC are difficult to select. Therefore, ENN is introduced into the control system to replace the switching control law of CSMC and estimate the lumped uncertainty. Experiments based on a digital signal processor (DSP), TMS320 F28335 show that

the proposed control method is effective. From the experimental results, the PMLSM servo system based on CSMC via ENN possesses the advantages of good tracking accuracy and robustness for the tracking of different reference trajectories.

II. MODEL OF PMLSM

PMLSM is an electromagnetic device that directly generates linear motion. It can be seen as a rotary motor which is cut along the radial direction and expanded the circumference into a straight line [26]. The structure of a rotary motor and a PMLSM is shown in Fig.1.
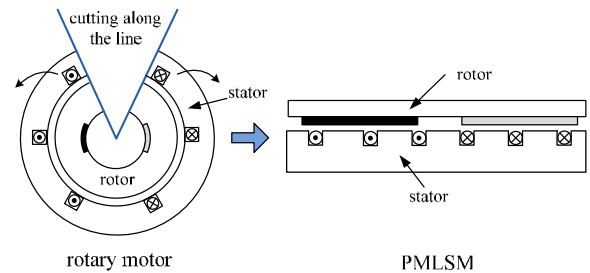

FIGURE 1. The structure of a rotary motor and a PMLSM.

With the implementation of field-oriented control, the electromagnetic thrust is simplified as

$$F_e = K_f i_q \tag{1}$$

$$K_f = 3\pi p_n \psi_f / 2\tau \tag{2}$$

where F_e is the electromagnetic thrust, K_f is the thrust coefficient, i_q is the q-axis current, p_n is the number of pole pairs, ψ_f is the magnet flux, τ is the pole pitch.

The mover dynamic equation of the PMLSM using the electromagnetic thrust shown in (1) can be

$$M\dot{v} = F_e - Bv - F_L \tag{3}$$

where M is the mass of the mover, B is the viscous friction coefficient; v is the linear velocity of the mover, F_L is lumped uncertainty including external disturbances, friction forces and parameter variations. In addition, friction forces consist of the static friction, Coulomb friction and vicious friction. The friction forces can be formulated as [27]

$$F_{fri} = \left[f_c + (f_m - f_c) e^{-(v/v_s)^2} \right] \text{sgn}(v) + Bv \tag{4}$$

where F_{fri} is the friction force, f_c is the Coulomb friction, f_m is the static friction, v_s is the Stribeck velocity, $\text{sgn}(\cdot)$ is a sign function.

The following equation can be obtained by substituting (1) into (3)

$$\dot{v} = -Bv/M + K_f i_q / M - F_L / M \tag{5}$$

III. PROPOSED CONTROL SYSTEM

In order to suppress the influence of the lumped uncertainty on the permanent magnet linear servo system and achieve high-precision tracking performance and strong robustness,
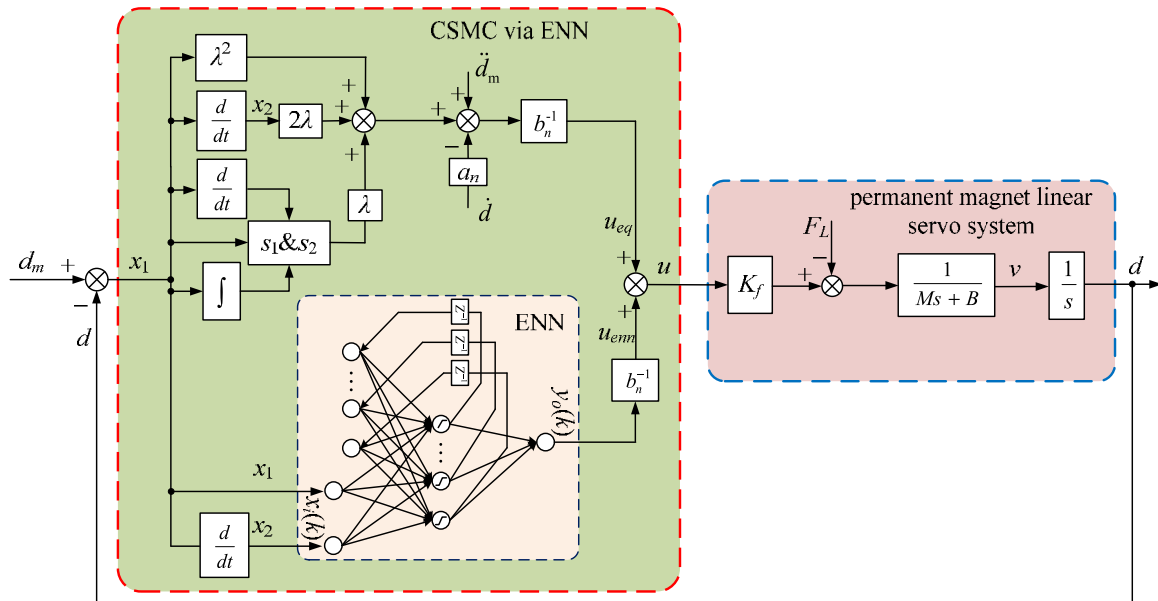
FIGURE 2. Structure diagram of CSMC via ENN for PMLSM servo system.

a control strategy combining CSMC with ENN is proposed. The structure diagram of CSMC via ENN for PMLSM servo system is shown in Fig.2.

A. CSMC DESIGN

To simplify the calculation, the following state variables are defined: $x_1 = d_m - d$, $x_2 = \dot{x}_1$. By using the mathematical model of PMLSM, the error state equation of PMLSM can be obtained

$$\begin{bmatrix} \dot{x}_1 \\ \dot{x}_2 \end{bmatrix} = \begin{bmatrix} 0 & 1 \\ 0 & a \end{bmatrix} \begin{bmatrix} x_1 \\ x_2 \end{bmatrix} + \begin{bmatrix} 0 \\ b \end{bmatrix} u + \begin{bmatrix} 0 \\ c \end{bmatrix} F_L \quad (6)$$

where $a = -B/M$, $b = K_f/M$, $c = -1/M$, $u = i_q$ is the control effort.

Considering the existence of the parameter variations, external disturbances and friction forces of the PMLSM servo system, the field-oriented control PMLSM servo system can be formulated as follows

$$\dot{x}_2 = (a_n + \Delta a) x_2 + (b_n + \Delta b) u + (c_n + \Delta c) F_L$$
$$= a_n x_2 + b_n u + \beta \quad (7)$$

where a_n, b_n, c_n are the nominal value of a, b, c, Δa, Δb, Δc denote the uncertainties introduced by system parameters M and B, $\beta = \Delta a x_2 + \Delta b u + (c_n + \Delta c) F_L$ is the lumped uncertainty, and β is assumed to be bounded

$$|\beta| \le \rho \quad (8)$$

where ρ is a given positive constant, and it is also considered as the switching control gain of CSMC.

Compared with SMC, CSMC has two sliding surfaces which are integral sliding surface and complementary sliding surface. The existence condition of sliding surface is that the system state point can reach the sliding surface in finite time.

When the state point is above the sliding surface, the control result should make the state point go down through the sliding surface. Conversely, when the state point is below the sliding surface, the control result should make the state point go up through the sliding surface [28]. Thus, the arrival condition of sliding mode is defined as

$$\lim_{s \to 0^+} \dot{s} < 0, \quad \lim_{s \to 0^-} \dot{s} > 0 \quad (9)$$

This means within the range of the sliding surface, the trajectory will reach the sliding surface in finite time and satisfy the local arrival condition. The equivalent form of the arrival condition is expressed as

$$s\dot{s} < 0 \quad (10)$$

In order to ensure the arrival within finite time and avoid asymptotic approximation, (10) can be modified as [29]

$$\begin{cases} \dot{s} > \varepsilon, & s < 0 \\ \dot{s} < \varepsilon, & s > 0 \end{cases} \quad \text{or} \quad s\dot{s} < -\varepsilon |s| \quad (11)$$

where $\varepsilon > 0$, which enables the system state point to reach the sliding surface in finite time.

In order to eliminate the steady-state error of the system, the integral of tracking error x_1 is introduced into switching function, and the integral sliding surface $s_1(x)$ is defined as

$$s_1(x) = \left(\frac{d}{dt} + \lambda \right)^2 \int_0^t x_1 d\tau \quad (12)$$

where λ is a given positive constant.

The following equation can be obtained by substituting (6)-(7) into (12) and taking the derivative

$$\dot{s}_1(x) = \ddot{x}_1 + 2\lambda \dot{x}_1 + \lambda^2 x_1$$
$$= \ddot{d}_m - a_n x_2 - b_n u - \beta + 2\lambda \dot{x}_1 + \lambda^2 x_1 \quad (13)$$

In CSMC, complementary sliding surface $s_2(x)$ is defined as follows

$$s_2(x) = \left(\frac{d}{dt} + \lambda\right)\left(\frac{d}{dt} - \lambda\right)\int_0^t x_1 d\tau \tag{14}$$

The following equation can be obtained by substituting (6)-(7) into (14)

$$\begin{aligned}\dot{s}_2(x) &= \ddot{x}_1 - \lambda^2 x_1 \\ &= \ddot{d}_m - a_n x_2 - b_n u - \beta - \lambda^2 x_1\end{aligned} \tag{15}$$

Corresponding to the same positive constant λ, the relationship between $s_1(x)$ and $s_2(x)$ can be obtained as follows

$$\sigma(x) = s_1(x) + s_2(x) \tag{16}$$

The following equation can be obtained by substituting (12) and (14) into (16)

$$\begin{aligned}\sigma(x) &= \left(\frac{d}{dt} + \lambda\right)^2 \int_0^t x_1 d\tau + \left(\frac{d}{dt} + \lambda\right)\left(\frac{d}{dt} - \lambda\right)\int_0^t x_1 d\tau \\ &= 2(\dot{x}_1 + \lambda x_1)\end{aligned} \tag{17}$$

The following equation can be obtained by using (13), (15) and (17)

$$\dot{s}_2(x) + \lambda\sigma(x) = \dot{s}_1(x) \tag{18}$$

In order to ensure the stability of the system, the first Lyapunov function candidate for the CSMC system is chosen as

$$V = \frac{1}{2}\left(s_1^2 + s_2^2\right) \tag{19}$$

The following equation can be obtained by taking the time derivative of (19) and using (13)-(15)

$$\begin{aligned}\dot{V} &= s_1 \dot{s}_1 + s_2 \dot{s}_2 \\ &= (s_1 + s_2)\left[\ddot{d}_m - a_n x_2 - b_n u - \beta + 2\lambda\dot{x}_i + \lambda^2 x_i - \lambda s_2\right]\end{aligned} \tag{20}$$

CSMC control law u is designed by using (20)

$$u = u_{eq} + u_v \tag{21}$$

$$u_{eq} = b_n^{-1}\left(\ddot{d}_m - a_n x_2 + 2\lambda\dot{x}_1 + \lambda^2 x_1 + \lambda s_1(x)\right) \tag{22}$$

$$u_v = b_n^{-1}\left[\rho\, sat\left(\frac{\sigma(x)}{\Phi}\right)\right] \tag{23}$$

where u_{eq} is the equivalent control law, u_v is the switching control law, Φ is the boundary layer thickness, and sat($\cdot$) is a saturation function, which is designed as follows

$$sat\left(\frac{\sigma(x)}{\Phi}\right) = \begin{cases} 1, & \sigma(x) \geq \Phi \\ \dfrac{\sigma(x)}{\Phi}, & -\Phi < \sigma(x) < \Phi \\ -1, & \sigma(x) \leq -\Phi \end{cases} \tag{24}$$

The following equation can be obtained by using (20)-(24)

$$\begin{aligned}\dot{V} &= s_1 \dot{s}_1 + s_2 \dot{s}_2 \\ &= (s_1 + s_2)(-B_n u_v) - \lambda(s_1 + s_2)^2 + (s_1 + s_2)(-\beta) \\ &\leq (s_1 + s_2)(-B_n u_v) - \lambda(s_1 + s_2)^2 + |s_1 + s_2|(|\beta|) \\ &\leq |s_1 + s_2|(|\beta| - \rho) - \lambda(s_1 + s_2)^2\end{aligned} \tag{25}$$

Due to $|\beta| \leq \rho$, $\dot{V} \leq 0$ can be obtained. Therefore, the system satisfies the Lyapunov stability condition. In other words, the system can converge to the boundary layer within any finite time [30]. The convergence trajectory of CSMC is shown in Fig.3.
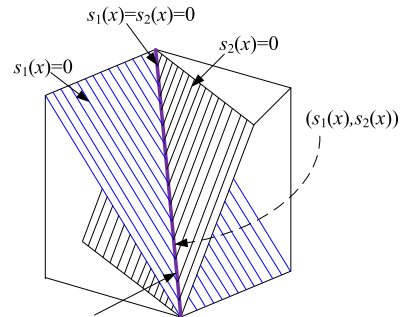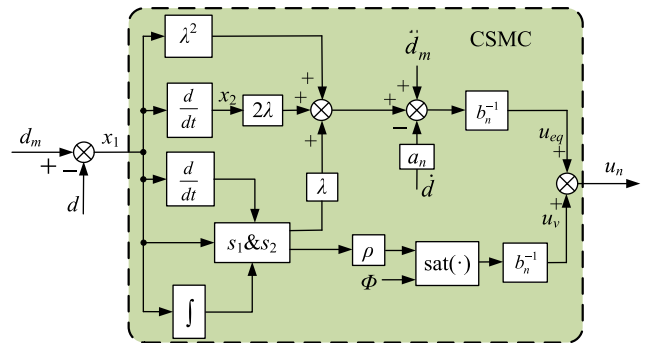

FIGURE 3. Convergence trajectory of CSMC.

FIGURE 4. Structure diagram of CSMC.

The structure diagram of CSMC is shown in Fig.4. In practical applications, it is difficult to measure the parameters of the system and the external disturbances, so the switching control gain ρ and the thickness of the boundary layer Φ are difficult to select the appropriate values. To reduce chattering and improve tracking accuracy of the PMLSM servo system, the value of ρ and Φ is usually chosen by the method of experience or trial.

B. ELMAN NEURAL NETWORK DESIGN

In order to solve the problem of parameter selection in CSMC and improve the system performance, a method combined CSMC with ENN is proposed. In the proposed method, ENN is used to replace the switching control in CSMC and estimate the lumped uncertainty of the PMLSM servo system. The control law u_n of the proposed method can be obtained as follows

$$u_n = u_{eq} + u_{enn} \tag{26}$$

$$u_{enn} = b_n^{-1} y_o(k) \tag{27}$$

where u_{enn} is the control law of the CSMC via ENN, $y_o(k)$ is the output of ENN, which is used to replace the function relation between ρ and Φ in (23). The structure diagram of
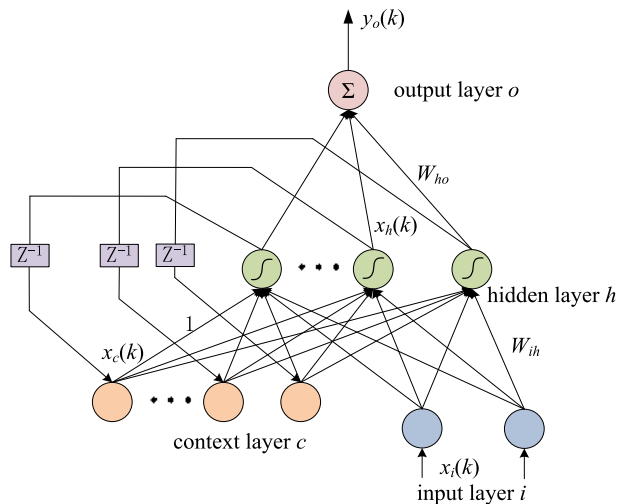
FIGURE 5. Structure diagram of ENN.

ENN is shown in Fig.5. ENN has two inputs and one output, which includes input layer, context layer, hidden layer and output layer. Compared with RBFNN, ENN has a context layer, which enables the network to have a strong ability to memory dynamic information. The signal propagation and the basic function in each layer of the ENN are introduced as follows.

1) LAYER 1. INPUT LAYER

In this layer, the input and the output of the node are represented as

$$x_i (k) = net_i, \quad i = 1, 2 \tag{28}$$

where net_i is the input of the ith node, $x_i (k)$ is the output of the ith node at the time of k.

2) LAYER 2. HIDDEN LAYER

In this layer, the input and the output of the node are represented as

$$x_h (k) = S (net_h) \tag{29}$$

$$S (net_h) = \frac{1}{1 + e^{-\lambda net_h}} \tag{30}$$

where net_h is the input of hidden layer, $x_h (k)$ is the output of hidden layer. S function is selected as the activation function of the hidden layer. The input of the hidden layer net_h contains two parts and it is represented as follows

$$net_h = \sum_c x_c (k) + \sum_i W_{ih} \times x_i (k) \tag{31}$$

where $\sum_c x_c (k)$ is the output of context layer, W_{ih} is the connective weight between input neurons and hidden neurons.

3) LAYER 3. CONTEXT LAYER

In this layer, the input and the output of the node are represented as

$$x_c (k) = x_h (k - 1) \tag{32}$$

where $x_h (k - 1)$ is the output of hidden layer at the time of $k - 1$, and it is also as the input of context layer at the time of k.

4) LAYER 4. OUTPUT LAYER

In this layer, the input and the output of the node are represented as

$$y_o (k) = net_o (k) \tag{33}$$

$$net_o (k) = \sum_h W_{ho} \times x_h (k) \tag{34}$$

where $y_o (k)$ is the output of this layer, W_{ho} is the connective weight between hidden neurons and output neurons.

In practical applications, the update of connective weight can be modified by static back propagation (BP) algorithm, but the output of ENN is not only related to the input of the time of k, but also related to the input of the time of $k - 1$. Therefore, the dynamic learning law is adopted when the accurate calculation results are required. The error function of the time of k is defined as follows

$$E (k) = \frac{1}{2} (d_m (k) - d (k))^2 = \frac{1}{2} e^2 (k) \tag{35}$$

The error term to be propagated is computed as

$$\delta_o = -\frac{\partial E}{\partial y_o (k)} = -\frac{\partial E}{\partial e} \frac{\partial e}{\partial y_o (k)} = -\frac{\partial E}{\partial e} \frac{\partial e}{\partial d} \frac{\partial d}{\partial y_o (k)} \tag{36}$$

The update law of the connective weight is defined as

$$W (k + 1) = W (k) + \Delta W (k) \tag{37}$$

where W is the connective weight of input layer, hidden layer and output layer.

The update of W_{ho} is defined as

$$\begin{aligned} \Delta W_{ho} &= -\eta_1 \times \frac{\partial E (k)}{\partial W_{ho}} \\ &= -\eta_1 \times \frac{\partial E (k)}{\partial y_o (k)} \times \frac{\partial y_o (k)}{\partial net_o (k)} \times \frac{\partial net_o (k)}{\partial W_{ho}} \\ &= -\eta_1 \times \delta_0 \times x_h (k) \end{aligned} \tag{38}$$

$$\delta_0 = \frac{\partial E (k)}{\partial y_o (k)} \tag{39}$$

where η_1 is the learning rate of W_{ho}.

The update of W_{ih} is defined as

$$\begin{aligned} \Delta W_{ih} &= -\eta_2 \times \frac{\partial E (k)}{\partial W_{ih}} \\ &= -\eta_2 \times \frac{\partial E (k)}{\partial y_o (k)} \times \frac{\partial y_o (k)}{\partial net_o (k)} \times \frac{\partial net_o (k)}{\partial W_{ho}} \times \frac{\partial x_h (k)}{\partial W_{io}} \\ &= -\eta_2 \times \delta_0 \times W_{ho} \times x_i (k) \end{aligned} \tag{40}$$

where η_2 is the learning rate of W_{ih}.

ENN can be trained by train function. The connective weights are calculated and adjusted by the BP algorithm of errors to complete online learning. By using (37) and (38), the training block diagram of the connection weight W_{ho} from hidden neurons to output neurons is shown in Fig.6. In the training process, the error gradient of the connective weight
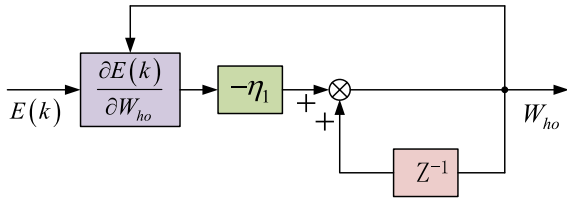
FIGURE 6. Training block diagram of W_{ho} from hidden neurons to output neurons.

can be determined by the BP algorithm of the error to adjust the connective weight.

The selection of the learning rate in neural network has a great influence on network performance. In order to train ENN effectively, discrete Lyapunov function is used to ensure error convergence. The convergence analysis of the network is as follows.

Define η_1 as the learning rate between hidden neurons and output neurons, and $P_{1\,\text{max}} = \max \|P_1(k)\|$, where $P_1(k) = \partial y_o / \partial W_{ho}$ and $\|\cdot\|$ is the Euclidean Norm defined on $\Re^n$. Assume $\eta_1 = \lambda/(P_{1\,\text{max}})^2 = \lambda/R_n$, where $0 < \lambda \le e^2(k)/(\delta_o + \varepsilon_o)$, R_n is the neurons of hidden layer, ε_o is a positive constant.

Proof: According to

$$P_1(N) = \frac{\partial y_o}{\partial W_{ho}} = \frac{\partial y_o}{\partial net_o} \times \frac{\partial net_o}{\partial W_{ho}} = x_h \qquad (41)$$

The following inequality can be obtained

$$\|P_1(N)\| < \sqrt{R_n} \qquad (42)$$

The discrete Lyapunov function is defined as follows

$$V(k) = \frac{1}{2}e^2(k) \qquad (43)$$

During adjacent sampling time, the Lyapunov function can be represented as

$$\Delta V(k) = V(k+1) - V(k) = \frac{1}{2}\left[e^2(k+1) - e^2(k)\right] \qquad (44)$$

The error can be described as

$$e(k+1) = e(k) + \Delta e(k) = e(k) + \left[\frac{\partial e(k)}{\partial W_{ho}}\right]^T \times \Delta W_{ho} \qquad (45)$$

where Δe and ΔW_{ho} are the variation of tracking error and connective weight, respectively. The following equation can be obtained by using (37), (38) and (45)

$$\begin{aligned}
&\|e(k+1)\| \\
&= \left\|e(k) + [(-1/e(k))\,\delta_o P_1(k)]^T [\eta_1 \delta_o P_1(k)]\right\| \\
&= \left\|e(k) + \left[1 - \eta_1(\delta_o/e(k))^2 P_1^T(k) P_1(k)\right]\right\| \\
&\le \|e(k)\|\left\|1 - \eta_1(\delta_o/e(k))^2 P_1^T(k) P_1(k)\right\| \qquad (46)
\end{aligned}$$

By using $\eta_1 = \lambda/(P_{1\,\text{max}})^2 = \lambda/R_n$ and $0 < \lambda \le e^2(k)/(\delta_o + \varepsilon_o)$, one can be obtained that

$\left\|1 - \eta_1(\delta_o/e(k))^2 P_1^T(k) P_1(k)\right\| < 1$. Consequently, $V > 0$ and $\dot{V} < 0$ are satisfied in the system by adopting Lyapunov stability theory. Thus, it can be implied that the tracking error will converge to zero as $t \to \infty$. Similarly, the tracking error of system will converge to zero under the specific network learning parameters [31].

IV. EXPERIMENTAL RESULTS
A. EXPERIMENT SYSTEM
To test the feasibility and the validity of the proposed method, a PMLSM servo system based on DSP, TMS320 F28335 experiment platform is set up in Fig.7. The control-based servo system consists of PMLSM, PC, DSP, intelligent power module (IPM) and detection units. The hardware structure diagram of PMLSM control system based on DSP is shown in Fig.8.
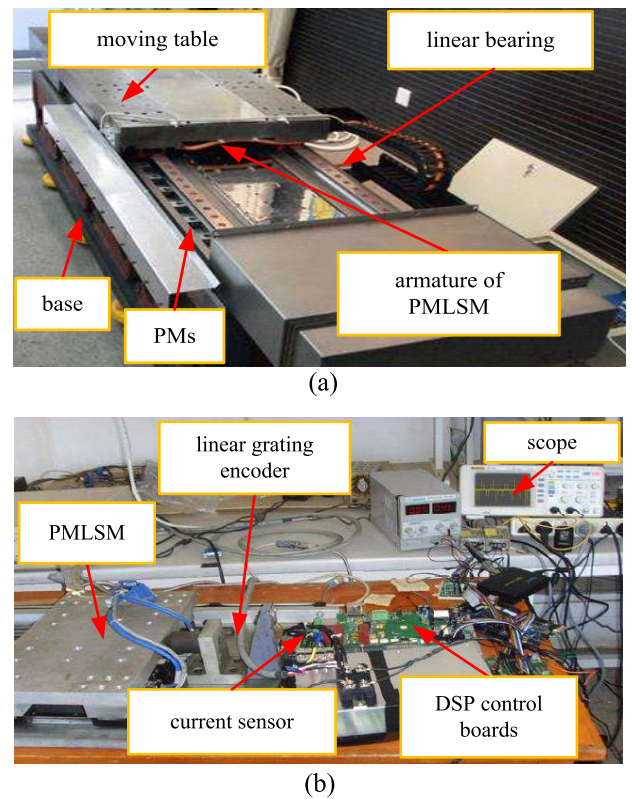

(a)

(b)

FIGURE 7. Experimental setup of control system. (a) The structure of PMLSM (b) PMLSM servo system based on DSP.

A detailed description of the PMLSM servo system based on DSP can be found as follows.

(1) PMLSM: The control object of the experimental system is the PMLSM produced by Kollmorgen, American, its maximum distance can be reached 260 mm.

(2) DSP: The control chip is TMS320 F28335 DSP with a sampling period 100 μs, which is specially designed for motor control with the peripheral circuit driven by a motor. Therefore, it is extremely suitable for the development of all-digital servo controller. Its operation speed can reach up
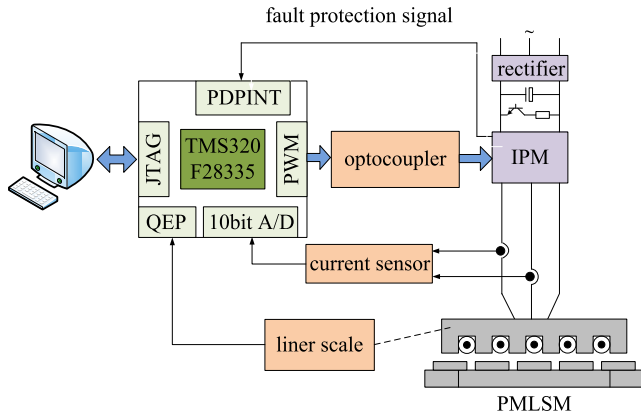
FIGURE 8. Hardware structure diagram of PMLSM control system based on DSP.

TABLE 1. Parameters of PMLSM.

Item and Symbol	Value
resistance R_s (Ω)	2.1
magnet flux Ψ_f (Wb)	0.09
inductance L_d / L_q (mH)	41.4
pole pitch τ(mm)	32
number of pole pairs	3
thrust coefficient K_f（N/A）	50.7
mover mass M (kg)	16.4
viscous friction coefficient B (N·s/m)	8.0

TABLE 2. Parameters in CSMC via ENN.

Item and Symbol	value
positive constant λ	60
switching control gain ρ	5
boundary thickness φ	0.0015
learning rate η_1	0.1
learning rate η_2	0.3
initial value of connective weights	0
neurons of input layer	2
neurons of hidden layer	9
neurons of context layer	9
neurons of output layer	1

to 30 MIPS, which makes it possible to implement some more complex modern control.

(3) IPM inverter: The power conversion unit is PS21865 IPM (20A/600V) produced by Mitsubishi, Japan. It has a built-in IGBT drive circuit, overload protection and power supply under-voltage protection function, all of those can contribute to the reliable operation of the system.

(4) Current detection unit: Three-phase current signals of PMLSM are obtained by LT 58-S7 Hall current sensors to constitute a current feedback control with a ratio of 1000:1.

(5) Linear grating sensor detection unit: A linear grating sensor with resolution 1 μm is used to detect position of the moving table. MicorE linear grating sensor is MII1600, which can directly pick up position signals and velocity signals, and offer feedback to the system.

The main PMLSM servo system parameters are given in Table 1.

The parameters in CSMC via ENN are given in Table 2. For the selection of parameters in CSMC, the trial and error method is adopted to obtain the best control performance by continuously debugging parameters, whereas in the proposed CSMC via ENN, ENN is used to replace the switching control law, thus avoiding the selection of parameters in CSMC. In addition, the selection of parameters in ENN mainly depends on the experience. In order to achieve the optimal transient and steady-state control performance, the parameters are selected to satisfy the stability requirements of the experiment.

B. LINEAR MOTION TRAJECTORY COMPARATIVE EXPERIMENTS

In order to verify the effectiveness of the proposed method, CSMC, CSMC via RBFNN, CSMC via ENN are implemented in the experimentation for the comparison of the control performance, respectively. Different from ENN, RBFNN is a static neural network with two inputs and one output. It contains input layer, hidden layer and output layer. The Gauss basis function is selected as the activation function of hidden layer. In addition, RBFNN has 2, 9 and 1 neurons at the input, hidden, and output layers, respectively. To verify the effectiveness of CSMC via ENN with different reference trajectories, external disturbances and parameter variations, experimental cases of permanent magnet linear servo system are shown in Table 3.

In case 1, a non-periodic trapezoidal signal is given as the reference trajectory. In the case of nominal parameters, some experimental results are provided to demonstrate the effectiveness of the proposed method. Fig.9 and Fig.10 are the position tracking curves and the tracking error curves of PMLSM servo system for non-periodic trapezoidal signals when using CSMC, CSMC via RBFNN and CSMC via ENN, respectively. By comparing these curves, it can be seen that the tracking error curves are almost invariant in a certain range during the rising and stable stages of the position, while at the turning points of the given trapezoidal signal, the tracking error curves fluctuate greatly, which is caused by the sudden change of v at the turning points and the existence of the system inertia. From Fig.10, it can be seen that the position tracking error based on CSMC is at the range of −2.0-12.5 μm, and the one under CSMC via RBFNN

TABLE 3. Experimental cases of permanent magnet linear servo system.

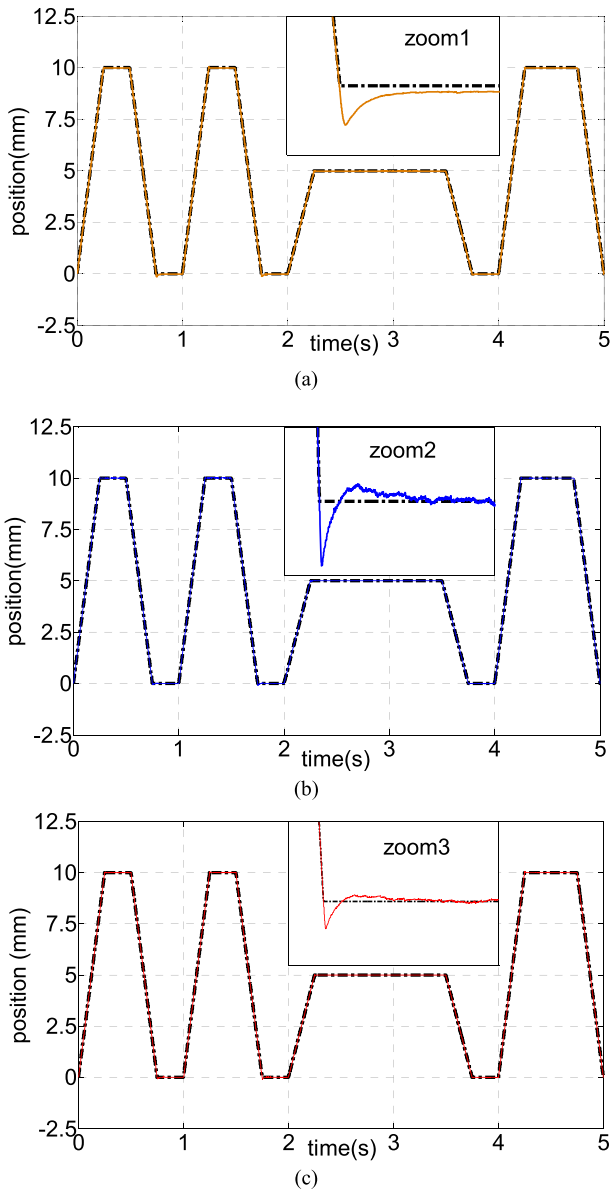|	Reference trajectory	External disturbance	Actual mover mass M_a	Actual viscous friction coefficient B_a
Case 1	trapezoidal	0 N	$M_a=M$	$B_a=B$
Case 2	sinusoidal	50 N	$M_a=M$	$B_a=B$
Case 3	sinusoidal	0 N	$M_a=2M$	$B_a=1.5B$

FIGURE 9. Position tracking curves of PMLSM servo system for non-periodic trapezoidal signals when using (a) CSMC (b) CSMC via RBFNN (c) CSMC via ENN.

FIGURE 10. Position tracking error curves of PMLSM control system for non-periodic trapezoidal signals when using (a) CSMC (b) CSMC via RBFNN (c) CSMC via ENN.

is about -3.2-9.0 μm. However, the position error curve under the control of the proposed method is approximately at the range of -1.8-6.0 μm. In addition, by observing the fluctuation of curves, it is found that the proposed method can effectively reduce chattering. Therefore, CSMC via ENN for
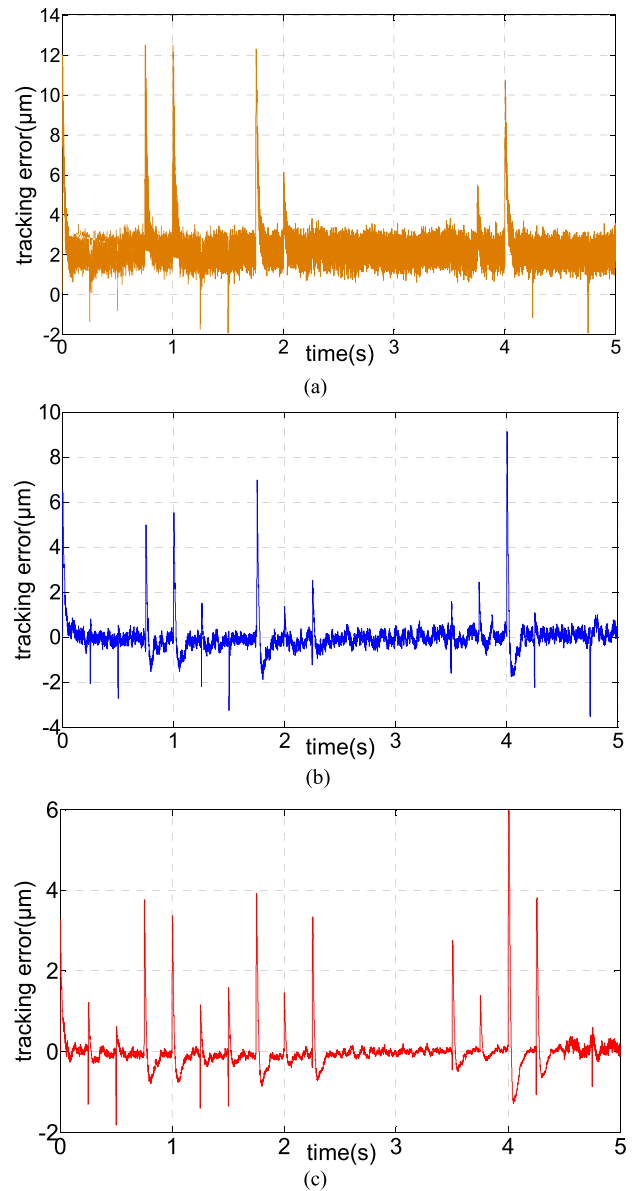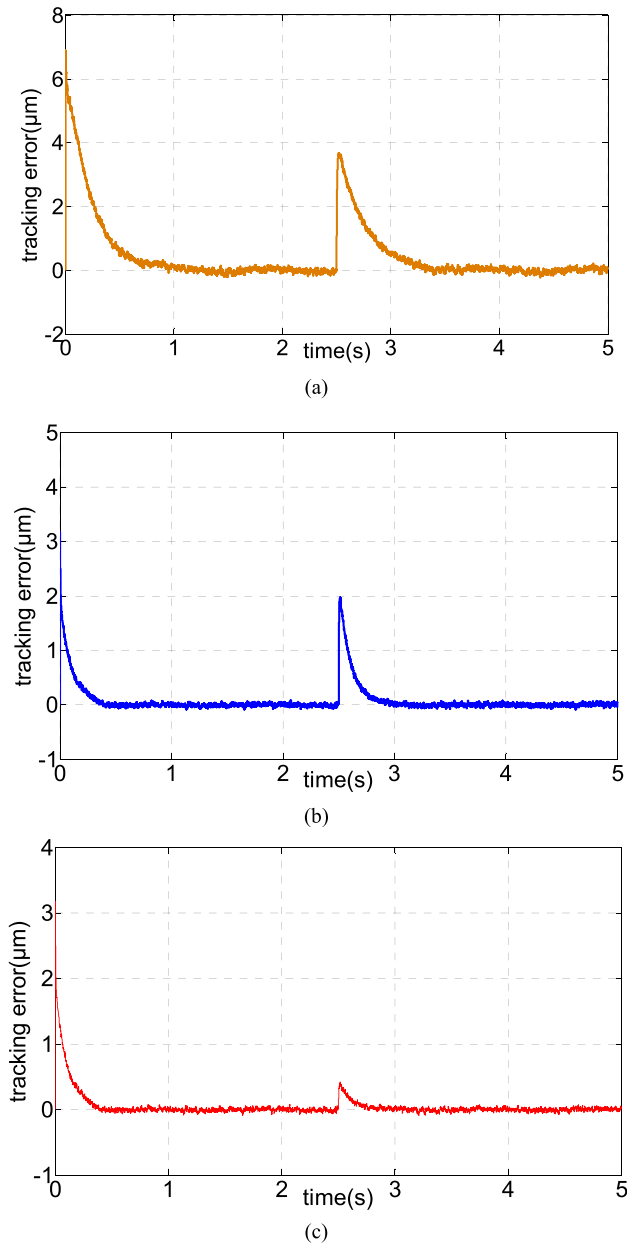
the PMLSM servo system has a good tracking performance among the three controllers.

In case 2, a sinusoidal input signal with a period of 2s and an amplitude of 10mm is given as a reference trajectory for the PMLSM servo system. 50N external disturbance is
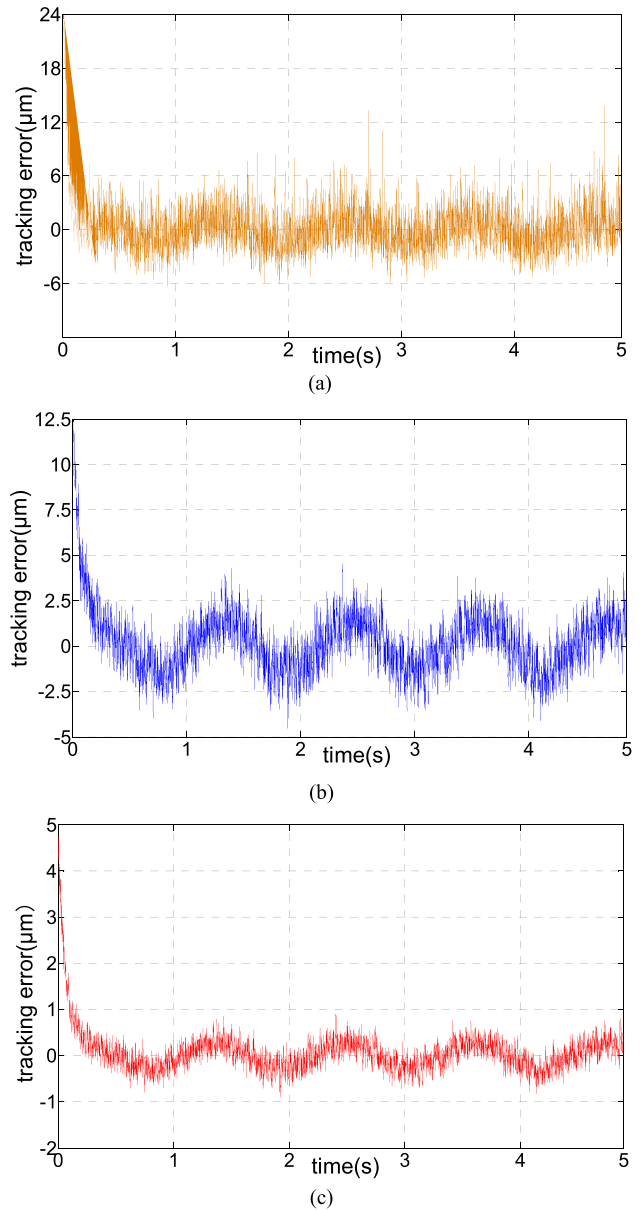
FIGURE 11. Position tracking error curves of PMLSM servo system with sudden external disturbance for sinusoidal signal when using (a) CSMC (b) CSMC via RBFNN (c) CSMC via ENN.

FIGURE 12. Position tracking error curves of PMLSM servo system with parameter variations for sinusoidal signal when using (a) CSMC (b) CSMC via RBFNN (c) CSMC via ENN.

applied to the system at the time of 2.5s. Fig.11 is the position tracking error curves of CSMC, CSMC via RBFNN, and the proposed method, respectively. By observing the error curves of PMLSM servo system under sudden external disturbance, it can be seen that the tracking error of CSMC via ENN is about 0.5 μm, which is 25%, 13% of the CSMC and CSMC via RBFNN. It shows that the proposed method can effectively suppress the influence of disturbances on the system, thereby enhancing the robustness of the system.

In case 3, under the condition of parameter variations, the PMLSM system is given the same reference trajectory as case 2. Since actual position response curves coincide

with the reference trajectory, only the position tracking error curves are shown in Fig.12 to verify the effectiveness of the control method. It can be seen from Fig.12 that the proposed method can also achieve precise position tracking when the parameters change.

In order to demonstrate the improvement of the proposed strategy clearly, a quantified data is given as follows. The performance measures of these three methods for the tracking of different cases are shown in Fig.13. From the bar chart of tracking error, it can be seen clearly that compared with CSMC and CSMC via RBFNN, the amplitude of tracking error is significantly reduced under the proposed method. Therefore, the effectiveness and necessity of CSMC via ENN are verified.
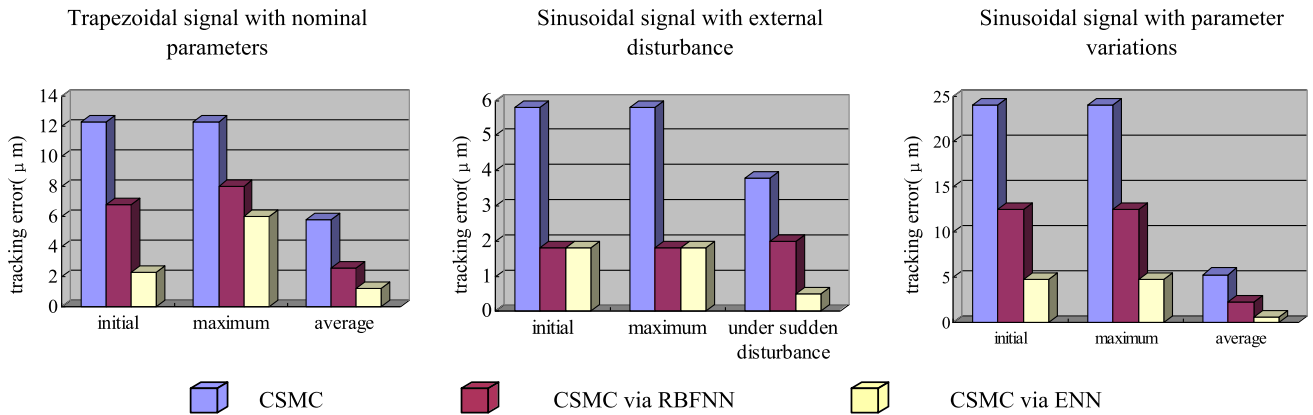
FIGURE 13. Performance measures of PMLSM servo system for different cases.

V. CONCLUSIONS

This paper has proposed a reliable control strategy for permanent magnet linear servo system, which can suppress the influence of the lumped uncertainty and provide satisfactory performance. By implementing DSP as the core control unit to control the mover of PMLSM for the tracking of different reference trajectories, the tracking performance and the robustness of the PMLSM servo system have been verified.

In addition, the proposed method can also be applied to the multi-axis motion system such as H-type gantry stage, dual linear motors and five-axis linkage motion system. For further works, the following issues are deserved to be considered.

(1) The sliding mode surfaces used in the paper can only guarantee the asymptotic convergence of the tracking errors. To improve the performance of the proposed CSMC via ENN in practice, the integral terminal sliding surfaces such as the one in [32], [33] should be used to guarantee the fast and finite-time convergence.

(2) In the designed controller, the friction force is considered as a part of the lumped uncertainty, and the influence of friction force on the system is not properly analyzed. In order to establish a more perfect controller, disturbance observer such as the one in [34] should be combined to further improve the system performance.

REFERENCES

[1] S.-Y. Chen and T.-S. Liu, "Intelligent tracking control of a PMLSM using self-evolving probabilistic fuzzy neural network," *IET Electr. Power Appl.*, vol. 11, no. 6, pp. 1043–1054, Feb. 2017.

[2] W.-T. Su and C.-M. Liaw, "Adaptive positioning control for a LPMSM drive based on adapted inverse model and robust disturbance observer," *IEEE Trans. Power Electron.*, vol. 21, no. 2, pp. 505–517, Mar. 2006.

[3] C.-C. Hwang, P.-L. Li, and C.-T. Liu, "Optimal design of a permanent magnet linear synchronous motor with low cogging force," *IEEE Trans. Magn.*, vol. 48, no. 2, pp. 1039–1042, Feb. 2015.

[4] C.-S. Ting, Y.-N. Chang, B.-W. Shi, and J.-F. Lieu, "Adaptive backstepping control for permanent magnet linear synchronous motor servo drive," *IET Electr. Power Appl.*, vol. 9, no. 3, pp. 265–279, 2015.

[5] M. Wang, L. Li, and D. Pan, "Detent force compensation for PMLSM systems based on structural design and control method combination," *IEEE Trans. Ind. Electron.*, vol. 62, no. 11, pp. 6845–6854, Nov. 2015.

[6] K. Cho and K. Nam, "Periodic learning disturbance observer based precision motion control in PMLSM motion systems considering long-term instability problem," *Int. J. Precis. Eng. Manuf.*, vol. 17, no. 9, pp. 1101–1112, Sep. 2016.

[7] F. Zhi, M. Zhang, Y. Zhu, and X. Li, "Analysis and elimination of harmonics in force of ironless permanent magnet linear synchronous motor," *Proc. CSEE*, vol. 37, no. 7, pp. 2101–2109, Apr. 2017.

[8] X. Zhao and J. Zhao, "Cross-coupled complementary sliding mode control for precision direct-drive gantry system," *Trans. China Electrotech. Soc.*, vol. 30, no. 11, pp. 7–12, Jun. 2015.

[9] C.-F. Hsu and T.-C. Kuo, "Intelligent complementary sliding-mode control with dead-zone parameter modification," *Appl. Soft Comput. J.*, vol. 23, no. 5, pp. 355–365, Oct. 2014.

[10] E.-J. Park, S.-Y. Jung, and Y.-J. Kim, "A design of optimal interval between armatures in long distance transportation PMLSM for end cogging force reduction," *J. Electr. Eng. Technol.*, vol. 11, no. 2, pp. 361–366, Mar. 2016.

[11] K. Kim, J. Kim, Y. M. Choi, and D. Gweon, "Hybrid control system for compensation of the force ripple in permanent magnet linear motor," *Adv. Sci. Lett.*, vol. 13, no. 1, pp. 132–136, Jun. 2012.

[12] P. G. Panah, M. Ataei, B. Mirzaeian, A. Kiyoumarsi, and A. Shafiei, "A robust adaptive sliding mode control for PMLSM with variable velocity profile over wide range," *Res. J. Appl. Sci. Eng. Technol.*, vol. 10, no. 9, pp. 997–1006, Oct. 2015.

[13] R. Shahnazi, H. M. Shanechi, and N. Pariz, "Position control of induction and DC servomotors: A novel adaptive fuzzy PI sliding mode control," *IEEE Trans Energy Convers.*, vol. 23, no. 1, pp. 138–147, Mar. 2008.

[14] X. Han, Q. Kun, and Z. Zhe, "Analysis and suppression measures of magnetic resistance force in permanent magnet linear synchronous motors," *Trans. China Electrotech. Soc.*, vol. 30, no. 6, pp. 70–76, Apr. 2015.

[15] V. Q. Leu, H. H. Choi, and J.-W. Jung, "Fuzzy sliding mode speed controller for PM synchronous motors with a load torque observer," *IEEE Trans. Power Electron.*, vol. 27, no. 3, pp. 1530–1539, Mar. 2012.

[16] B. Sun, X. Ge, and Y. Sun, "Dynamical integral sliding mode control for permanent magnet ring torque motor," *Adv. Mater. Res.*, vols. 383–390, pp. 799–804, Nov. 2011.

[17] L. Wu and X. Su, "Sliding mode control with bounded $\mathcal{L}_2$ gain performance of Markovian jump singular time-delay systems," *Automatica*, vol. 48, no. 8, pp. 1929–1933, Aug. 2012.

[18] C.-F. J. Kuo, C.-H. Hsu, and C.-C. Tsai, "Control of a permanent magnet synchronous motor with a fuzzy sliding-mode controller," *Int. J. Adv. Manuf. Technol.*, vol. 32, no. 7, pp. 757–763, Apr. 2007.

[19] M. Roopaei, M. Zolghadri, and S. Meshksar, "Enhanced adaptive fuzzy sliding mode control for uncertain nonlinear systems," *Commun. Nonlinear Sci. Numer. Simul.*, vol. 14, nos. 9–10, pp. 3670–3681, Sep. 2009.

[20] F.-J. Lin, P.-H. Shieh, and P.-H. Shen, "Robust recurrent-neural-network sliding-mode control for the X-Y table of a CNC machine," *IEEE Proc.-Control Theory Appl.*, vol. 153, no. 1, pp. 111–123, Feb. 2006.

[21] J. Fei and C. Lu, "Adaptive fractional order sliding mode controller with neural estimator," *J. Franklin Inst.*, vol. 355, no. 5, pp. 2369–2391, 2018.

[22] J. Fei and X. Liang, "Adaptive backstepping fuzzy neural network fractional-order control of microgyroscope using a nonsingular terminal sliding mode controller," *Complexity*, vol. 2018, Sep. 2018, Art. no. 5246074.

[23] J.-P. Su and C.-C. Wang, "Complementary sliding control of non-linear systems," *Int. J. Control*, vol. 75, no. 5, pp. 360–368, Nov. 2002.

[24] X. Zhao and J. Zhao, "Complementary sliding mode variable structure control for permanent magnet linear synchronous motor," *Proc. CSEE*, vol. 35, no. 10, pp. 2552–2557, May 2015.

[25] F.-J. Lin, J.-C. Hwang, P.-H. Chou, and Y.-C. Hung, "FPGA-based intelligent-complementary sliding-mode control for PMLSM servo-drive system," *IEEE Trans. Power Electron.*, vol. 25, no. 10, pp. 2573–2587, Oct. 2010.

[26] M.-Y. Chen and J.-S. Lu, "High-precision motion control for a linear permanent magnet iron core synchronous motor drive in position platform," *IEEE Trans Ind. Informat.*, vol. 10, no. 1, pp. 99–108, Feb. 2014.

[27] Y. Tan, J. Chang, and H. Tan, "Adaptive backstepping control and friction compensation for AC servo with inertia and load uncertainties," *IEEE Trans. Ind. Electron.*, vol. 50, no. 5, pp. 944–952, Oct. 2003.

[28] N. T.-T. Vu, D.-Y. Yu, H. H. Choi, and J.-W. Jung, "T–S fuzzy-model-based sliding-mode control for surface-mounted permanent-magnet synchronous motors considering uncertainties," *IEEE Trans. Ind. Electron.*, vol. 60, no. 10, pp. 4281–4291, Nov. 2013.

[29] J. Liu, *Advanced Sliding Mode Control for Mechanical Systems*. Beijing, China: Science Press, 2017, pp. 6–8.

[30] J. Slotine and W. Li, *Applied Nonlinear Control*. Upper Saddle River, NJ, USA: Prentice-Hall, 1991, pp. 276–306.

[31] F.-J. Lin, S.-Y. Chen, K.-K. Shyu, and Y.-H. Liu, "Intelligent complementary sliding-mode control for lusms-based X-Y-Θ motion control stage," *IEEE Trans. Ultrason., Ferroelectr., Freq. Control*, vol. 57, no. 7, pp. 1626–1640, Jul. 2010.

[32] L. Qiao and W. Zhang, "Adaptive non-singular integral terminal sliding mode tracking control for autonomous underwater vehicles," *IET Control Theory Appl.*, vol. 11, no. 8, pp. 1293–1306, Feb. 2017.

[33] L. Qiao and W. Zhang, "Double-loop integral terminal sliding mode tracking control for UUVs with adaptive dynamic compensation of uncertainties and disturbances," *IEEE J. Ocean. Eng.*, vol. 44, no. 1, pp. 29–53, Jan. 2019.

[34] R. Yang, M. Wang, L. Li, Y. Zenggu, and J. Jiang, "Integrated uncertainty/disturbance compensation with second-order sliding-mode observer for PMLSM-driven motion stage," *IEEE Trans. Power Electron.*, vol. 34, no. 3, pp. 2597–2607, Mar. 2019.

HONGYAN JIN was born in Shenyang, Liaoning, China, in 1993. She received the B.S. degree in electrical engineering from the Shenyang University of Technology, Shenyang, in 2016, where she is currently pursuing the Ph.D. degree in electrical engineering. Her research interests include motor control and intelligent control.

XIMEI ZHAO was born in Changchun, Jilin, China, in 1979. She received the B.S., M.S., and Ph.D. degrees in electrical engineering from the Shenyang University of Technology, Shenyang, China, in 2003, 2006, and 2009, respectively, where she is currently a Professor and a Doctoral Supervisor with the School of Electrical Engineering. Her research interests are electrical machines, motor drives, motor control, intelligent control, and robot control. She has authored or coauthored over 100 technical papers, three textbooks, and holds 15 patents in these areas.

• • •